THE JOURNAL OF PHYSICAL CHEMISTRY C

Article

Cite This: J. Phys. Chem. C 2018, 122, 24760−24764

pubs.acs.org/JPCC

Ice Nucleation at the Water−Sapphire Interface: Transient Sum-Frequency Response without Evidence for Transient Ice Phase

Ahmed Abdelmonem,*[,†] Ellen H. G. Backus,[‡] and Mischa Bonn*[,‡]

[†]Institute of Meteorology and Climate Research—Atmospheric Aerosol Research (IMKAAF), Karlsruhe Institute of Technology (KIT), 76344 Eggenstein-Leopoldshafen, Germany

[‡]Max Planck Institute for Polymer Research, Ackermannweg 10, 55128 Mainz, Germany

Supporting Information

ABSTRACT: Heterogeneous ice nucleation at the water−sapphire interface is studied using sum-frequency generation spectroscopy. We follow the response of the O−H stretch mode of interfacial water during ice nucleation as a function of time and temperature. The ice and liquid states each exhibit very distinct, largely temperature-independent responses. However, at the moment of freezing, a transient response with a significantly different intensity is observed, with a lifetime between several seconds and several minutes. The presence of this transient signal has previously been attributed to a transient phase of ice. Here, we demonstrate that the transient signal can be explained without invoking a transient ice phase, as the transient signal can simply be accounted for by a linear combination of time-dependent liquid and ice responses.

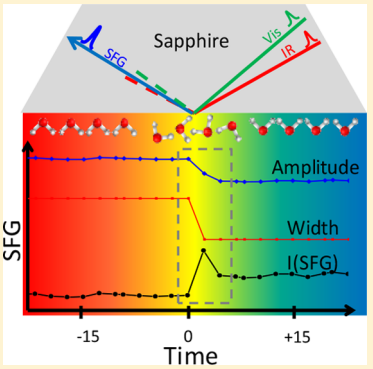

INTRODUCTION

The liquid−ice phase transition of water plays a major role in many processes on our globe. Important examples include glacier melting on earth and heterogeneous ice nucleation on atmospheric aerosols which have been linked to the formation, microphysics, and optical properties of clouds. Understanding the details of this phase transformation is essential for a manifold of not only atmospheric but also environmental and food science-related disciplines.

The transformation of water to ice is generally triggered by nucleation at the surface of particles, and as such, understanding the liquid−solid transformation of water in contact with the surface of relevant materials is of great interest to several disciplines. Owing to its surface specificity and its sensitivity to the molecular organization of water molecules at buried interfaces, sum-frequency generation (SFG) spectroscopy has recently been intensely used to study water freezing at solid surfaces.[1−5] In SFG spectroscopy,[6,7] infrared (IR) and visible (VIS) laser beams are overlapped at the interface, and the sum-frequency of the two incident beams can be generated. As this is a second-order nonlinear optical method, the signal is forbidden in centrosymmetric media like bulk water and proton-disordered hexagonal ice, the most common form of ice in the biosphere under standard atmospheric conditions. However, at the interface, the symmetry is broken, making the interface SFG-active. If, moreover, the IR beam is in resonance with a molecular vibration, the signal is enhanced. In this way, the vibrational spectrum of the interfacial water molecules could be obtained during heterogeneous ice nucleation. The technique relies on the OH stretch vibration of water changing substantially upon crystallization of water.

With this method, Anim-Danso et al. have reported a transient signal upon water freezing next to a mica surface[4] and at the sapphire surface at high pH (=9.8)[1] during their investigations of water freezing next to solid surfaces in the pH range from 3.3 to 9.8. They attributed the transient signal to events taking place near the surface during the ice formation and ice melting. More recently, Lovering et al.[3] reported a transient SFG signal during ice nucleation of neutral water at silica surfaces. The transient signal was attributed to the existence of a transient phase of stacking-disordered ice during the freezing process at water−mineral interfaces. The stacking-disordered ice at the water−silica interface was reported at a temperature ∼20 °C higher than the temperature at which it is observed in bulk ice.[3] It was therefore concluded in ref 3 that the mineral surface might play a role in promoting and stabilizing the formation of stacking-disordered ice at the interface. Both SFG studies showed a transient increase in the signal, albeit with different temporal characteristics (several minutes for a neutral water−silica interface[3] and a few tens of seconds for a pH 9.8 solution−sapphire interface[1]). Such a transient signal with a lifetime around 1 min has also been observed in a recent study on immersion freezing next to a mica surface using second harmonic generation spectroscopy.[8]

Here, we report similar transient signals in a SFG study of water freezing in contact with a sapphire α-$Al_2O_3(0001)$ surface for solutions with different pH values and thus different surface charges of the substrate. In agreement with the

Received: August 2, 2018
Revised: October 9, 2018
Published: October 10, 2018

DOI: 10.1021/acs.jpcc.8b07480
J. Phys. Chem. C 2018, 122, 24760−24764

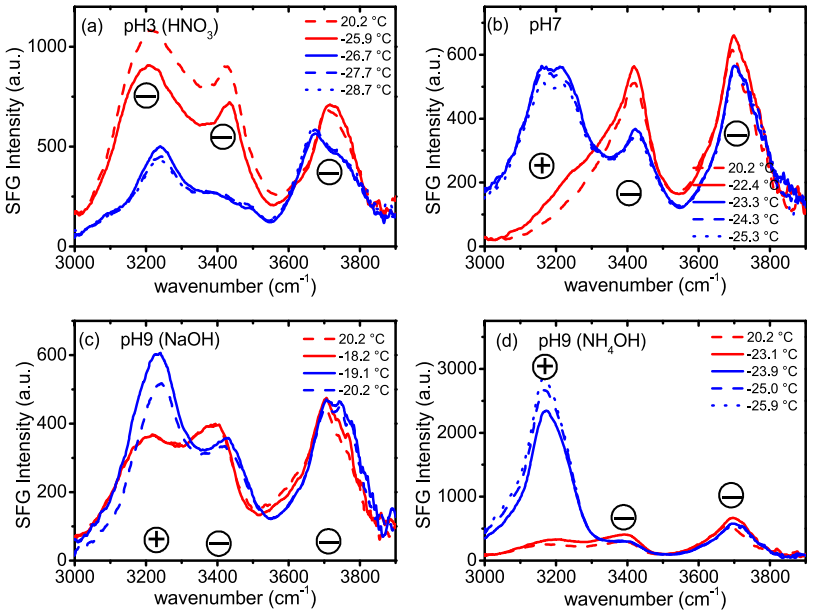

Figure 1. Measured SFG spectra of α-Al_2O_3 (0001)/water interfaces collected in SSP polarization during the cooling cycles of (a) pH 3—HNO_3, (b) pH 7, (c) pH 9—NaOH, and (d) pH 9—NH_4OH. The spectra shown here are Fresnel-corrected and present only those at room temperature (solid red lines), at freezing points (solid blue lines), and around the phase transition (nonsolid lines, red for liquid and blue for ice). The signs of the resonances are indicated by a circle with + or − sign and are taken from phase-resolved SFG experiments of ref 17. Non-Fresnel corrected SFG spectra are shown in Figure S1.

literature,[1,3,8] we confirm the existence of a transient signal at pH 7 and pH 9 and extend the study to low pH. However, the freezing temperatures we observed in our work are substantially lower compared to those observed by Anim-Danso et al. and Lovering et al.,[1,3] which indicates that nucleation was not occurring at the solid−liquid interface in those previous studies. Here, we ensure that we study specifically heterogeneous freezing at the sapphire−water interface by isolating a water drop using silicon oil.[5] By fitting the data, we show that the transient in the SFG signal intensity observed at specific frequencies during the freezing process can be explained without including a transient ice species: a model of two states, that is, liquid and solid, is sufficient to explain the observation.

EXPERIMENTAL SECTION

A detailed description of the experimental setup to perform SFG experiments while freezing a droplet can be found in Abdelmonem et al.[5] In brief, a custom-designed sample cell was used to probe the water− and ice−sapphire interface at different temperatures and pH values. A roughly 15 μL water drop was placed on the surface and isolated using silicon oil to avoid early freezing at different interfaces and to prevent partial evaporation of the water. Femtosecond IR and spectrally narrowed VIS pulses are mixed at a sapphire prism−water (or prism−ice) interface in a copropagating, total internal reflection geometry from the prism side to generate the SFG light. The reflected SFG light is spectrally dispersed by a monochromator and detected by an electron-multiplied charge-coupled device (Andor Technologies). The sapphire prism sample is placed in a copper adaptor which is fixed on a silver block, constituting the cooling/heating element of a Linkam cold-stage. A detailed description and drawing of the assembly of the measuring Teflon cell can be found in ref 8. The sample is cooled down stepwise at a rate of 1 °C per minute and a step size of 1 °C. At each integer of degree, the temperature is held constant for 1.5 min, and then, a spectrum is collected. The acquisition time per spectrum is 30 s. The freezing point is defined as the point when a visual inspection using a camera reveals that the droplet is frozen. The different experiments were repeated 3−5 times.

The spectra presented here are corrected for the frequency-dependent IR Fresnel factor, calculated following ref 9. Unfortunately, the complex refractive indices, which are required to evaluate the IR Fresnel coefficients, of ice and liquid water have been reported in the literature only for specific temperatures. We use the IR refractive indices of liquid water at −20 °C,[10] which is close to the transition temperature in our SFG experiments. For ice, we use the values reported by the same author at −38 °C,[10] which is the closest temperature to the transition points in our experiments. The refractive index of sapphire is calculated from the Sellmeier equation.[11] The spectra reported here were taken under SSP polarization combination (S-polarized SFG and VIS; P-polarized IR). After Fresnel correction, the spectra are directly proportional to the surface nonlinear susceptibility tensor for SSP polarization $|\chi^{(2)}_{yyz}|^{(2)}$. To separate contributions from different resonant features in SFG, the $|\chi^{(2)}_{yyz}|^{(2)}$ spectra were fit with a sum of a nonresonant contribution, with amplitude A_0 and phase φ, and a sum of Lorentzian peaks representing the resonant contributions

$$|\chi^{(2)}_{yyz}|^{(2)} = |\chi^{(2)}_{NR} + \chi^{(2)}_{R}|^{(2)} = \left| A_0\, e^{i\phi} + \sum_q \frac{A_q}{\omega_{IR} - \omega_q + i\Gamma_q} \right|^{(2)} \quad (1)$$

where A_q, ω_q, and $2\Gamma_q$ are the amplitude, frequency, and full width half-maximum linewidth of the qth vibrational resonance, respectively. More details about the data analysis

DOI: 10.1021/acs.jpcc.8b07480
J. Phys. Chem. C 2018, 122, 24760−24764

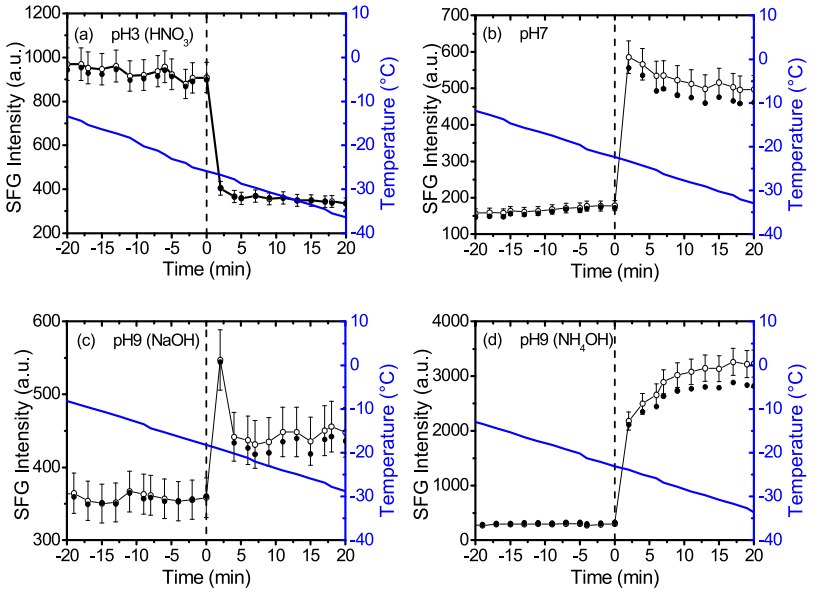

Figure 2. Fresnel-corrected measured SFG intensity (black solid circles) and intensity of the fit (black lines with open circles) for the four sets of spectra of the four pH solutions as a function of time at a fixed wavenumber (3200 cm^{-1}). The blue line shows the change in temperature with time during the cooling process. The error bars have been evaluated from the standard deviation of five measurements of the signal at 3200 cm^{-1} at room temperature for a NH_4OH solution.

and Fresnel factor corrections can be found in the Supporting Information of Abdelmonem et al.[5] Several examples of the fitting results around the freezing point (time zero) are shown in Figure S2 to demonstrate the fit quality.

RESULTS AND DISCUSSION

Figure 1 shows a selection of Fresnel factor-corrected SFG intensity spectra for SSP polarization combination for the liquid and ice phase measured for the pH 3 (HNO_3), pH 7, pH 9 (NaOH), and pH 9 (NH_4OH) solutions in contact with the sapphire (0001) surface. The non-Fresnel-corrected spectra are plotted in Figure S1. Given that the point of zero charge of the sapphire (0001) surface is between pH = 5.3 and 7.3,[12−17] the chosen range of pHs allows to investigate freezing at positive (low pH), near-neutral (neutral pH), and negative (high pH) surface charge. Upon decreasing the temperature from room temperature to the freezing point, the SFG spectra are more or less constant. The freezing process begins at ∼−26.7, −23.3, −19.1, and −23.9 °C for pH 3 (HNO_3), pH 7, pH 9 (NaOH), and pH 9 (NH_4OH), respectively, in this particular set of experiments. Because ice nucleation is a stochastic process, the "real" onset temperature for freezing has to be determined with droplet freezing assay measurements. The results for the systems mentioned above have been reported in Abdelmonem et al.[5] The freezing temperatures we obtained in our work are substantially lower than those reported in refs.[1,3,18] This can be attributed to the methodology used here: the isolation of the probed water drop with oil prevents ice nucleation at locations other than the water−sapphire interface.

Figure 1a−d shows spectra at room temperature (solid red lines) and around the liquid−ice transition (dashed red for liquid and blue lines for ice) for pH 3, pH 7, pH 9 (NaOH), and pH 9 (NH_4OH), respectively. For all samples, the liquid water signal underwent a gradual change at the surface from room temperature to right above the freezing point and to then change dramatically upon freezing. At low pH, a substantial decrease in the signal upon freezing is followed by a further slower decrease. For pH 7 and 9, the signal around 3200 cm^{-1} increases substantially upon crystallization, especially for pH 9 (NH_4OH). The observation for the pH 9 (NH_4OH) solution is in good agreement with ref 4.

To illustrate the dynamics of the freezing process, we plot in Figure 2 the SFG intensity at a fixed wavenumber, 3200 cm^{-1}, for the four pH solutions, as a function of time as done by Anim-Danso et al.[1] and Lovering et al.[3] As is clear from Figure 2, the intensity at 3200 cm^{-1} is more or less constant upon cooling until freezing. The freezing point can be clearly recognized by the sudden change (increase or decrease) in the SFG intensity around time zero. After freezing, the intensity is also constant upon further cooling down. For pH 3, the SFG intensity at 3200 cm^{-1} is lower after the freezing event, whereas for the other cases, the signal for the ice state is higher than that for the liquid state. Moreover, around the phase transition from liquid to solid, the spectral intensity at 3200 cm^{-1} is transiently higher for pH 9 (NaOH) and pH 7. For pH 9 (NH_4OH), we observe that the spectral intensity at 3200 cm^{-1} is growing in the first minutes after freezing before it reaches a stable value. This means that we observe a transient lower signal than that observed for the ice state. The different behavior for NaOH and NH_4OH both in the spectral shape in Figure 1 and the transient behavior in Figure 2 are likely due to contributions from NH vibrational modes and/or ion-specific effects. The results are in qualitative agreement with the results of Lovering et al.[3] on the neutral surface and Anim-Danso et al.[1] on the negatively charged surface, respectively, although the transient intensity is significantly lower. The lower intensity can be attributed to a difference in time resolution: our full spectra are acquired in 2 min intervals, whereas Lovering et al. reported only the 3200 cm^{-1} intensity but with a resolution of 5 s.

As we observe a transient signal for pH 9 with NaOH and pH 7 in the absence of ions, the presence of ions cannot be the cause of the transient signal, although it may affect the dynamics.

DOI: 10.1021/acs.jpcc.8b07480
J. Phys. Chem. C 2018, 122, 24760−24764

Table 1. Central Frequency (in cm^{-1}) of Each Band for all Solutions[a]

peak label	peak 1 position/linewidth		peak 2 position/linewidth		peak 3 position/linewidth	
origin	strongly hydrogen bonded water		weakly hydrogen bonded water		surface hydroxyl (Al_2OH)	
	phase					
solution	liquid	ice	liquid	ice	liquid	ice
pH 3 (HNO_3)	3226/107	3248/75	3411/84	3401/97	3695/65	3677/86
pH 7	3172/132	3166/105	3441/65	3470/47	3705/82	3725/71
pH 9 (NaOH)	3158/110	3207/84	3427/72	3470/54	3715/91	3738/83
pH 9 (NH_4OH)[a]	3149/121	3171/61	3422/54	3442/36	3699/67	3718/46

[a]For pH 9 (NH_4OH), the OH bands likely also contain a contribution from the NH deformation and symmetric stretch modes. These are not considered explicitly because the individual contributions from these modes are not directly apparent from the recorded spectra.

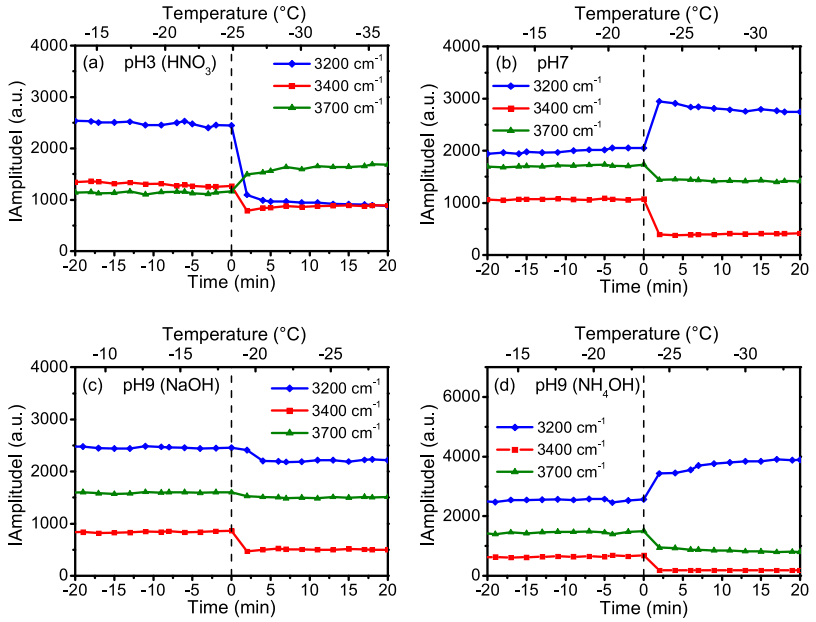

Figure 3. Absolute peak amplitude of individual bands for all solutions.

To characterize the temperature-dependent spectra quantitatively, we fit all data using a sum of a nonresonant contribution and three Lorentzian lineshapes—see eq 1. Following ref 5, we fit the spectra using three peaks around 3200, 3400, and 3700 cm^{-1}, which have been assigned to, respectively, strongly and weakly hydrogen-bonded interfacial water and surface hydroxyl (Al_2OH) groups. For simplicity, the peaks are labeled 3200, 3400, and 3700 cm^{-1}.[17,19−21] A detailed discussion of these bands can be found in ref 5 and references therein.

To investigate the temporal changes in the signal, we fit the spectra at all different temperatures. Although describing the spectra by three resonances is clearly an approximation [e.g., for pH 3 (HNO_3), a shoulder on the high-frequency part of the 3700 peak is apparent after freezing], the quality of the fits is consistently good (see Supporting Information). The center frequencies and linewidths of the resonances were kept constant for each phase (liquid and ice) in the fit procedure. Moreover, the nonresonant amplitude and phase are kept at 4 and 5, respectively, for all samples in both the liquid and ice phase. Table 1 shows the peak position and linewidth (Γ) of each band.

Figure 3 shows the area (i.e., A_q from eq 1) of each band as a function of temperature. A_q represents the integrated area of the Im[$\chi^{(2)}$] band associated with the vibration, which provides a measure of the population associated with that band. Figure 3 shows that all band amplitudes are constant for the liquid phase up to the freezing point, at which point a sudden drop or increase is observed and to then stabilize again at a different level for ice. Comparing the time dependence of the 3200 peak amplitudes with the measured SFG intensities at 3200 cm^{-1} (Figure 2), we see notably different transient shapes. The anomalous behavior observed for the SFG intensity shown in Figure 2, for example, a temporary overshoot of the SFG intensity especially for pH 9 (NaOH), is not apparent from the time-dependent amplitudes (A_q) of the modes shown in Figure 3.

It is therefore apparent that the transient signals observed in Figure 2b,c can be well accounted for by a smooth transition between two states (water and ice), without the need for invoking a transient species. The transient intensity signals in Figure 2 can be accounted for by a subtle interference between different peak parameters, changing at slightly different rates, which have a combined effect on the overall intensity (see eq 1). To exclude that the results are depending on the fitting routine, we performed fit procedures with different constraints. The results are plotted in Figure S3. In the first additional fitting routine, the nonresonant amplitude and phase were not globally constraint but still constant within a certain phase (liquid−ice) like the frequencies and linewidths of the resonances. The second additional fit procedure has no constraints. The different fit routines result in subtle changes

DOI: 10.1021/acs.jpcc.8b07480
J. Phys. Chem. C 2018, 122, 24760−24764

but do not affect the conclusions drawn in this manuscript. Specifically, in our spectral analysis, we also find no evidence for a transient increase or decrease in the central frequency, which one would expect if a transient ice phase were formed.

CONCLUSIONS

The effect of surface charge on the rearrangement of the interfacial water molecule at the sapphire (0001) surface after immersion freezing has been studied on the molecular level using SFG spectroscopy of supercooled water. The surface charge was varied between positive, neutral, and negative by changing the solution pH of an isolated droplet placed on the surface. All solutions showed distinct transients in the intensity signal, however, with different trends. A detailed analysis of the Fresnel-corrected temperature-dependent spectra reveals that a discrete transition from water to ice is sufficient to explain the observed transients.

ASSOCIATED CONTENT

Supporting Information

The Supporting Information is available free of charge on the ACS Publications website at DOI: 10.1021/acs.jpcc.8b07480.

Examples of the SFG spectra fitting (PDF)

AUTHOR INFORMATION

Corresponding Authors

*E-mail: ahmed.abdelmonem@kit.edu (A.A.).
*E-mail: bonn@mpip-mainz.mpg.de (M.B.).

ORCID

Ahmed Abdelmonem: 0000-0002-4348-2439
Ellen H. G. Backus: 0000-0002-6202-0280
Mischa Bonn: 0000-0001-6851-8453

Notes

The authors declare no competing financial interest.

ACKNOWLEDGMENTS

A.A. is grateful to the German Research Foundation (DFG, AB 604/1-1,2). E.H.G.B. thanks the ERC (Starting grant no. 336679). The authors are grateful to M. Alejandra Sánchez, Jenée D. Cyran, Marc-Jan van Zadel, Alexei Kiselev and Thomas Leisner for their support and useful discussions.

REFERENCES

(1) Anim-Danso, E.; Zhang, Y.; Alizadeh, A.; Dhinojwala, A. Freezing of Water Next to Solid Surfaces Probed by Infrared-Visible Sum Frequency Generation Spectroscopy. *J. Am. Chem. Soc.* **2013**, *135*, 2734−2740.

(2) Anim-Danso, E.; Zhang, Y.; Dhinojwala, A. Freezing and Melting of Salt Hydrates Next to Solid Surfaces Probed by Infrared-Visible Sum Frequency Generation Spectroscopy. *J. Am. Chem. Soc.* **2013**, *135*, 8496−8499.

(3) Lovering, K. A.; Bertram, A. K.; Chou, K. C. Transient Phase of Ice Observed by Sum Frequency Generation at the Water/Mineral Interface During Freezing. *J. Phys. Chem. Lett.* **2017**, *8*, 871−875.

(4) Anim-Danso, E.; Zhang, Y.; Dhinojwala, A. Surface Charge Affects the Structure of Interfacial Ice. *J. Phys. Chem. C* **2016**, *120*, 3741−3748.

(5) Abdelmonem, A.; Backus, E. H. G.; Hoffmann, N.; Sánchez, M. A.; Cyran, J. D.; Kiselev, A.; Bonn, M. Surface-charge-induced orientation of interfacial water suppresses heterogeneous ice nucleation on α-alumina (0001). *Atmos. Chem. Phys.* **2017**, *17*, 7827−7837.

(6) Shen, Y. R. Surface Properties Probed by Second-Harmonic and Sum-Frequency Generation. *Nature* **1989**, *337*, 519−525.

(7) Wei, X.; Miranda, P. B.; Zhang, C.; Shen, Y. R. Sum-Frequency Spectroscopic Studies of Ice Interfaces. *Phys. Rev. B: Condens. Matter Mater. Phys.* **2002**, *66*, 085401.

(8) Abdelmonem, A. Direct molecular-level characterization of different heterogeneous freezing modes on mica - Part 1. *Atmos. Chem. Phys.* **2017**, *17*, 10733−10741.

(9) Zhuang, X.; Miranda, P. B.; Kim, D.; Shen, Y. R. Mapping Molecular Orientation and Conformation at Interfaces by Surface Nonlinear Optics. *Phys. Rev. B: Condens. Matter Mater. Phys.* **1999**, *59*, 12632−12640.

(10) Zasetsky, A. Y.; Khalizov, A. F.; Earle, M. E.; Sloan, J. J. Frequency Dependent Complex Refractive Indices of Supercooled Liquid Water and Ice Determined from Aerosol Extinction Spectra. *J. Phys. Chem. A* **2005**, *109*, 2760−2764.

(11) Malitson, I. H. Refraction and Dispersion of Synthetic Sapphire. *J. Opt. Soc. Am.* **1962**, *52*, 1377−1379.

(12) Fitts, J. P.; Shang, X.; Flynn, G. W.; Heinz, T. F.; Eisenthal, K. B. Electrostatic Surface Charge at Aqueous/α-Al2O3Single-Crystal Interfaces as Probed by Optical Second-Harmonic Generation. *J. Phys. Chem. B* **2005**, *109*, 7981−7986.

(13) Franks, G. V.; Meagher, L. The Isoelectric Points of Sapphire Crystals and Alpha-Alumina Powder. *Colloids Surf., A* **2003**, *214*, 99−110.

(14) Kershner, R. J.; Bullard, J. W.; Cima, M. J. Zeta Potential Orientation Dependence of Sapphire Substrates. *Langmuir* **2004**, *20*, 4101−4108.

(15) López Valdivieso, A.; Reyes Bahena, J. L.; Song, S.; Herrera Urbina, R. Temperature effect on the zeta potential and fluoride adsorption at the α-Al2O3/aqueous solution interface. *J. Colloid Interface Sci.* **2006**, *298*, 1−5.

(16) Veeramasuneni, S.; Yalamanchili, M. R.; Miller, J. D. Measurement of Interaction Forces between Silica and α-Alumina by Atomic Force Microscopy. *J. Colloid Interface Sci.* **1996**, *184*, 594−600.

(17) Zhang, L.; Tian, C.; Waychunas, G. A.; Shen, Y. R. Structures and Charging of α-Alumina (0001)/Water Interfaces Studied by Sum-Frequency Vibrational Spectroscopy. *J. Am. Chem. Soc.* **2008**, *130*, 7686−7694.

(18) Abdelmonem, A.; Lützenkirchen, J.; Leisner, T. Probing Ice-Nucleation Processes on the Molecular Level using Second Harmonic Generation Spectroscopy. *Atmos. Meas. Tech.* **2015**, *8*, 3519−3526.

(19) Sung, J.; Shen, Y. R.; Waychunas, G. A. The Interfacial Structure of Water/Protonated α-Al2O3 (1120) as a Function of pH. *J. Phys.: Condens. Matter* **2012**, *24*, 124101.

(20) Liu, D.; Ma, G.; Xu, M.; Allen, H. C. Adsorption of Ethylene Glycol Vapor on α-Al2O3(0001) and Amorphous SiO2Surfaces: Observation of Molecular Orientation and Surface Hydroxyl Groups as Sorption Sites. *Environ. Sci. Technol.* **2005**, *39*, 206−212.

(21) Rey, R.; Møller, K. B.; Hynes, J. T. Hydrogen Bond Dynamics in Water and Ultrafast Infrared Spectroscopy. *J. Phys. Chem. A* **2002**, *106*, 11993−11996.

DOI: 10.1021/acs.jpcc.8b07480
J. Phys. Chem. C 2018, 122, 24760−24764